Journal of Solid State Chemistry 192 (2012) 390–393

Contents lists available at SciVerse ScienceDirect

Journal of Solid State Chemistry

journal homepage: www.elsevier.com/locate/jssc

Neutron diffraction study of monoclinic brannerite-type CoV_2O_6

Mikael Markkula, Angel M. Arevalo-Lopez, J. Paul Attfield *

Centre for Science at Extreme Conditions and School of Chemistry, University of Edinburgh, Mayfield Road, Edinburgh EH9 3JZ, United Kingdom

ARTICLE INFO

Article history:
Received 6 March 2012
Received in revised form
13 April 2012
Accepted 15 April 2012
Available online 3 May 2012

Keywords:
Transition metal oxides
Magnetic order
Neutron diffraction

ABSTRACT

A variable-temperature powder neutron diffraction study of the monoclinic brannerite-type CoV_2O_6 (space group $C2/m$, $a=9.2531(2)$, $b=3.5040(1)$, $c=6.6201(1)$ Å and $\beta=111.617(1)^\circ$ at 300 K) is reported. No structural transition is observed down to 4 K, but a magnetostriction accompanying antiferromagnetic order at $T_N=15$ K is discovered. Antiferromagnetic order observed below T_N has an $a\times b\times 2c$ supercell in which Co^{2+} moments of magnitude 4.77(4) μ_B at 4 K lie in the ac plane and are ferromagnetically coupled within chains of edge-sharing CoO_6 octahedra parallel to b. Ferromagnetic chains are coupled antiferromagnetically to neighbouring chains in the a and c directions, and a model for the interchain order in the reported 1/3 magnetization plateau region is proposed.

1. Introduction

The magnetic properties of low-dimensional materials are of continuing interest as they enable fundamental theories and models to be tested. Metamagnetism and magnetization plateaus are among the unusual properties of low-dimensional magnetic oxides based on spin-3/2 ions such as Co^{2+}. 1/3 (of ferromagnetic) magnetization plateaus have been predicted and observed experimentally in spin-3/2 antiferromagnetic uniform chains [1,2] and are known to occur also in spin-3/2 ferromagnetic uniform chains [3].

The magnetic properties of brannerite type MV_2O_6 transition metal vanadates (M=Mn [4–6], Co [6–9], Ni [6,7], Cu [6,7,10–13]) have been widely studied. Their structures are based on that of the mineral brannerite, UTi_2O_6, which crystallises in monoclinic space group $C2/m$. CoV_2O_6 has monoclinic and triclinic brannerite type polymorphs, which are both one-dimensional materials with high spin Co^{2+} in edge-sharing chains of CoO_6 octahedra along the b-axis, connected by chains of VO_6 octahedra in the monoclinic structure, and by VO_6 octahedra and VO_4 tetrahedra in the triclinic phase. The V^{5+} ions have been described as being 5+1 coordinated in monoclinic brannerites because the sixth oxygen atom is weakly bonded at distances of 2.4–2.8 Å [14].

A recent study [15] reported monoclinic CoV_2O_6 to have an antiferromagnetic transition at $T_N\approx 15$ K. Two field induced transitions were found: to a 1/3 magnetisation plateau between 1.9 and 3.2 T, and a metamagnetic transition to full saturation magnetisation at 4 T, both measured at 1.8 K. The saturation moment of 4.5 μ_B at 5 K and 4 T was considerably larger than the expected spin-only value of 3 μ_B, for high spin Co^{2+}, indicating a significant orbital contribution to the moment.

Magnetisation and neutron scattering measurements for the triclinic CoV_2O_6 phase have recently been reported [3,15]. Similar transitions to the monoclinic form were found; an antiferromagnetic transition at $T_N=6.3$ K; onset of 1/3 magnetisation plateau at 0.36 T and a transition at 0.59 T to full magnetisation, both at 2 K [3]. Inelastic neutron scattering showed that the magnetic excitations above T_N, are deconfined solitons rather than the static spin reversals predicted for a uniform ferromagnetic Ising spin chain. Below T_N, a ladder of states due to the confining effect of the spin order was found, with weak confinement at $5\text{ K}<T<T_N$ which may correspond to a crossover between two- and three-dimensional magnetic ordering. However, powder neutron diffraction showed that the low temperature magnetic order was incommensurate and the full spin structure was not reported [3].

We report here a variable temperature powder neutron diffraction study of monoclinic CoV_2O_6 which has been carried out to discover whether the spin order is complex like that in the triclinic polymorph, or is commensurate like that in monoclinic MnV_2O_6 [4].

2. Experimental

A 3 g polycrystalline sample of monoclinic CoV_2O_6 was synthesised by grinding stoichiometric quantities of cobalt (II) acetate tetrahydrate (Aldrich, 99.99%) and V_2O_5 (Aldrich, 99.99%) in a mortar and then heating in a furnace in air. The sample was heated for 16 h at 650 °C and then for 48 h at 725 °C, followed by quenching in liquid nitrogen. Quenching is needed to avoid formation of the triclinic form—laboratory powder x-ray diffraction using Cu K_α radiation showed that only monoclinic CoV_2O_6

* Corresponding author. Fax: +44 131 650 4743.
E-mail address: j.p.attfield@ed.ac.uk (J. Paul Attfield).

0022-4596/$ - see front matter © 2012 Elsevier Inc. All rights reserved.
http://dx.doi.org/10.1016/j.jssc.2012.04.029

was present in the sample. Magnetic susceptibility data were recorded using a Quantum Design SQUID magnetometer.

Powder neutron diffraction patterns from the 3 g monoclinic CoV_2O_6 sample were measured using the high-resolution time-of-flight neutron diffractometer HRPD at the ISIS spallation source. Data were collected at 4 K, 10–50 K in 5 K intervals, and 60–300 K in 20 K intervals and were normalised using the MantidPlot program. Crystal and magnetic structures were refined using the GSAS software package [16].

3. Results

The nuclear diffraction intensities were fitted well by refining the structure in space group $C2/m$, as shown in Fig. 1, and no significant improvements were obtained by lowering the symmetry to acentric $C2$ as was originally reported for monoclinic CoV_2O_6 [8]. Small spurious peaks at d-spacings of 1.1, 1.3, 1.8 and 2.1 Å are seen in the profile from the $2\theta=90^\circ$ detector bank, but not in the backscattering ($2\theta=168^\circ$) data, showing that the additional peaks are from parasitic scattering in the 90° detector flightpath rather than an impurity phase. Possible Co/V inversion disorder was investigated but the cation sites were found to be fully occupied to within 2% experimental uncertainties. Refined atomic coordinates, lattice and thermal displacement parameters and selected interatomic distances from 4 to 300 K refinements are reported in Tables 1 and 2. Bond valence sums derived from the 300 K distances in Table 2 using standard $Co^{2+}-O$ and $V^{5+}-O$ parameters [17] are Co 1.96; V 5.24; O(1) 2.09; O(2) 2.01; and O(3) 2.12. The proximity of these values to the formal valences indicates that the crystal structure is accurately determined and is relatively unstrained despite the distorted octahedral coordinations around the two cation sites.

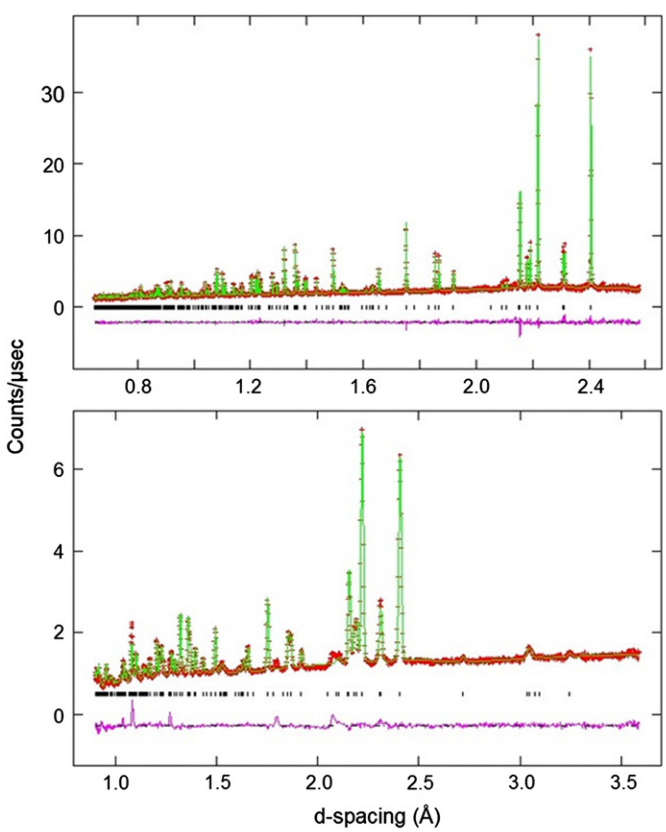

Fig. 1. Fitted time-of-flight neutron diffraction profiles for monoclinic CoV_2O_6 at 300 K. The upper and lower plots are respectively from the backscattering ($2\theta=168^\circ$) and 90° detector banks of instrument HRPD.

Table 1
Refined lattice parameters, atomic coordinates, and thermal displacement parameters from refinement of the CoV_2O_6 structure in monoclinic space group $C2/m$ at 4 (lower values) and 300 K (upper values). Fitting residuals, R_{wp}, and χ^2, were 0.044 and 3.60 at 4 K and 0.044 and 3.53 at 300 K.

a (Å)	b(Å)	c (Å)	β(°)	Volume (Å^3)
9.2531(2)	3.5040(1)	6.6201(1)	111.617(1)	199.545(5)
9.2291(1)	3.5027(1)	6.5972(1)	112.084(0)	197.616(5)
Atom	x	y	z	U_{iso} (Å^2)
Co	0	0	0	0.0090(10)
				0.0069(8)
V	0.3055(19)	0.5	0.3388(26)	0.0090(10)
	0.3090(18)		0.3430(24)	0.0069(8)
O(1)	0.1536(2)	0.5	0.1131(3)	0.0110(6)
	0.1536(2)		0.1105(3)	0.0070(4)
O(2)	0.4640(2)	0.5	0.2744(4)	0.0110(6)
	0.4667(2)		0.2779(3)	0.0070(4)
O(3)	0.1916(2)	0.5	0.5622(4)	0.0110(6)
	0.1912(2)		0.5620(3)	0.0070(4)

Table 2
Selected interatomic distances (Å) for monoclinic CoV_2O_6 from refinements at 4 and 300 K. Mean distances are shown as <M–O>.

	4 K	300 K
Co–O(1) × 4	2.198(2)	2.206(2)
Co–O(2) × 2	1.969(2)	1.964(2)
<Co–O>	2.084(2)	2.085(2)
V–O(1)	1.660(15)	1.631(16)
V–O(2)	1.665(16)	1.671(17)
V–O(2)	2.578(15)	2.661(15
V–O(3)	2.110(15)	2.110(17)
V–O(3) × 2	1.860(5)	1.867(6)
<V–O>	1.956(12)	1.968(13)

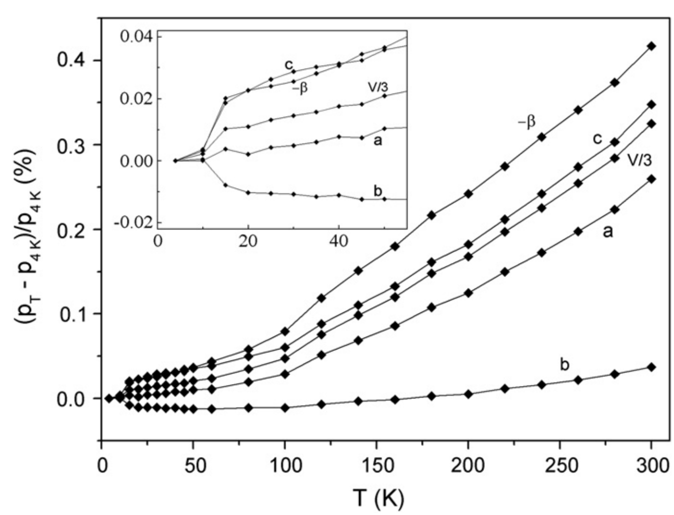

Fig. 2. Plot of lattice parameter changes against temperature for monoclinic CoV_2O_6. $\Delta p/p=(p_T-p_{4K})/p_{4K}$ changes are shown for crystallographic parameters $p=a$, b, c, $-\beta$ and V/3 (the latter is used for ease of comparison against the cell lengths). Changes are relative to the 4 K values shown in Table 1. Inset expansion shows the changes below 50 K.

No structural phase transitions were observed in monoclinic CoV_2O_6 between 4 and 300 K, but a magnetostriction has been discovered below the $T_N=15$ K magnetic ordering temperature. The anomaly is observed in all of the lattice parameters as shown in Fig. 2. The main changes are an anomalous increase in the b-axis length, parallel to the chains of edge-sharing CoO_6 octahedra, and decreases in c, the monoclinic angle (plotted as -β), and the

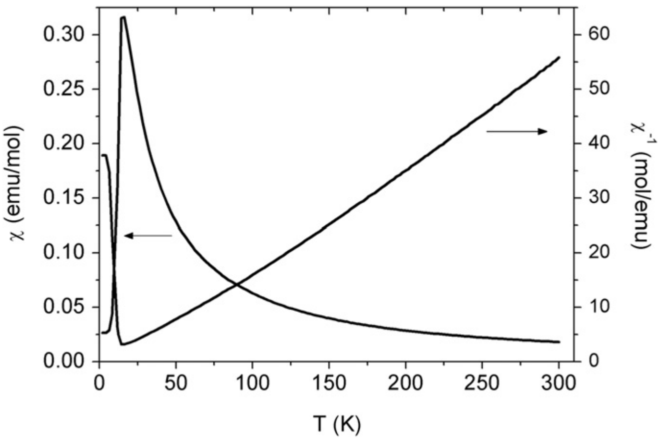

Fig. 3. Magnetic susceptibility and inverse susceptibility measurements for monoclinic CoV_2O_6 in a 1 T field.

cell volume as CoV_2O_6 is cooled below 15 K (T_N). This evidences a strong coupling of the spin order to the lattice.

Magnetic susceptibility measurements (Fig. 3) show monoclinic CoV_2O_6 to be a Curie–Weiss paramagnet at high temperatures and to have an antiferromagnetic transition at T_N=15 K. The inverse susceptibility curvature above T_N reveals short range antiferromagnetic fluctuations, but a fit to inverse susceptibility data between 280 and 300 K gives a fitted Weiss temperature of θ=42.1 K which shows that the strongest exchange interactions are ferromagnetic. The fitted paramagnetic moment of 6.09 μ_B is considerably larger than the spin-only value for high spin Co^{2+} of 3.87 μ_B, indicating that there is a large orbital contribution.

Magnetic diffraction peaks appear in neutron diffraction patterns below 15 K as shown in Fig. 4a. These are indexed by the (0 0 1/2) propagation vector and no additional incommensurate peaks were observed. A good fit to the magnetic intensities (Fig. 4b) was obtained using a collinear antiferromagnetic model in magnetic group *C* '2'/*m*' applied to the $a \times b \times 2c$ magnetic supercell. Co^{2+} moments lie in the *ac*-plane. The refined *a*, *c* and resultant moment values are μ_a=2.20(8), μ_c=4.24(6) and μ=4.77(4) μ_B at 4 K; and μ_a=2.12(10), μ_c=3.97(10) and μ=4.50(5) μ_B at 10 K. The resultant values are in good agreement with the saturation moment of 4.5 μ_B reported from high field magnetization measurements at 5 K [15]. The orbital contribution to the Co^{2+} moment in monoclinic CoV_2O_6 is unusually large although other examples of ordered moments in excess of the spin-only value of 3 μ_B are reported, e.g., 3.5 μ_B in $BiCoOPO_4$ [18] and 3.4 and 3.8 μ_B in $Co_2(OH)PO_4$ [19]. The crystal and magnetic structures of monoclinic CoV_2O_6 are shown in Fig. 5. Moments are approximately perpendicular to *a* in the *ac*-plane and are ferromagnetically coupled within the chains of edge-sharing CoO_6 octahedra parallel to *b*. Ferromagnetic chains are coupled antiferromagnetically to neighbouring chains in the *a* and *c* directions.

4. Discussion

This neutron diffraction study confirms that monoclinic CoV_2O_6 adopts the *C*2/*m* brannerite structure, with no significant cation disorder between Co and V sites in a sample quenched from 725 °C. No structural phase transitions are observed between 4 and 300 K, but the structure shows a magnetostrictive anomaly at the T_N=15 K magnetic transition. This is most likely due to spin–orbit effects at the high spin Co^{2+} ions which couple the spin–order to the lattice. The large orbital contributions to the high temperature paramagnetic and low temperature ordered moments support this conclusion. The magnetostriction expands

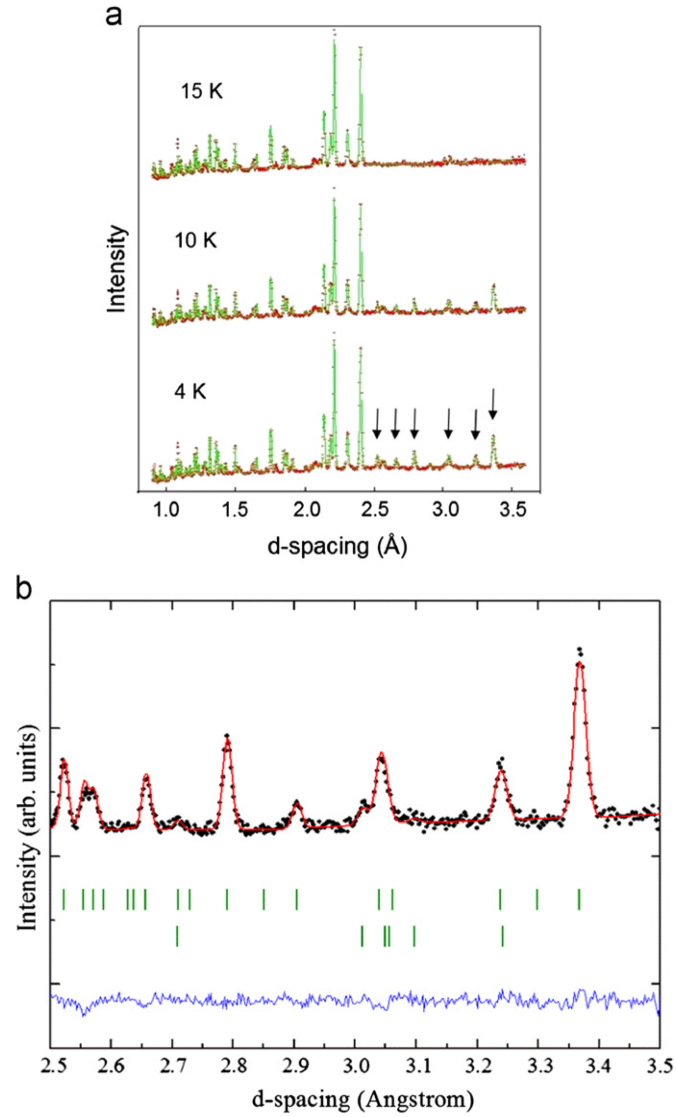

Fig. 4. Time-of-flight powder neutron diffraction profiles from the HRPD 90° detector for monoclinic CoV_2O_6 at 4, 10 and 15 K revealing magnetic peaks (arrowed) at the two lowest temperatures. Rietveld fits of the crystal and magnetic structure models are shown. (b) Expansion of the 4 K fit showing crystal/magnetic structure reflection markers as lower/upper tick marks, and the difference between observed and calculated profiles below.

the lattice in the direction of the ferromagnetically ordered Co^{2+} chains on cooling, but decreases the interchain distances slightly resulting in an overall volume contraction.

A strong spin–orbit coupling is also evidenced by the substantial tetragonal compression of the CoO_6 octahedra which have four long (2.21 Å) and two short (1.96 Å) Co–O bonds (see Table 2). A Jahn–Teller distortion, quenching the orbital moment, would require tetragonal elongation resulting in four short and two long bonds. The VO_6 octahedra are highly distorted, having two short (1.63 and 1.67 Å) V–O bonds in a cis-configuration with long (2.11 Å) and very long (2.66 Å) bonds opposite. This is equivalent to an off-centre displacement of V in the *ac*-plane, relative to the center of the VO_6 octahedron. These V^{5+} d°-cation displacements are antiferroelectrically ordered in the non-polar *C*2/*m* CoV_2O_6 structure.

The magnetic structure of monoclinic CoV_2O_6 has the same (0 0 1/2) order of spins as was found in isostructural MnV_2O_6 [4], although in that material the spins are parallel to *b* whereas they

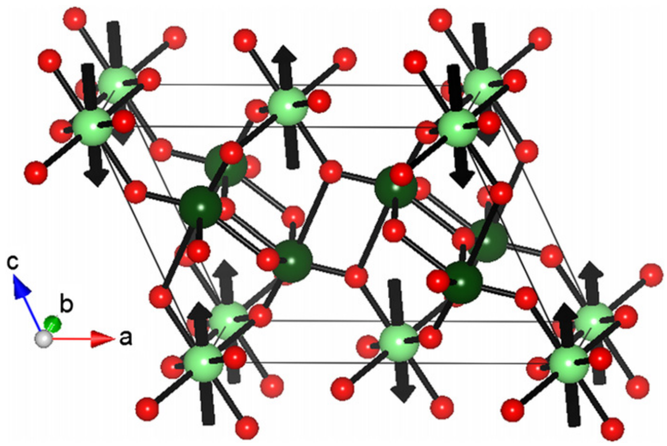

Fig. 5. The crystal and magnetic structures of monoclinic CoV_2O_6 shown for the nuclear *C*2/*m* cell with arrows indicating the ordered magnetic moment directions at the Co^{2+} ions. Co/V are shown are large light/dark spheres, and O are small spheres.

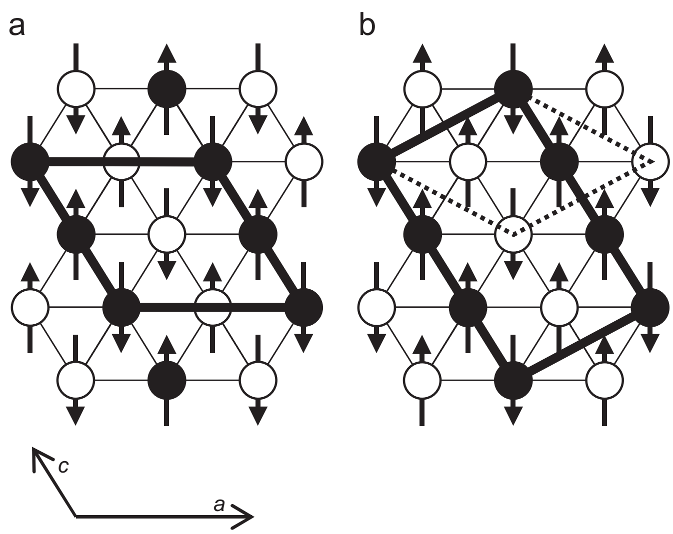

Fig. 6. Projections of the spin ordered chains in monoclinic CoV_2O_6 onto the *ac*-plane, transformed onto a hexagonal lattice. In this representation the *a* and *c* cell vectors are related as $a/c=2$ and $\beta=120^{\circ}$, whereas the actual values are $a/c=1.4$ and $\beta=112^{\circ}$. Co atoms at $y=0$ and 1/2 are shown as closed and open circles respectively. (a) shows the observed zero-field antiferromagnetic order with the $a\times b\times 2c$ magnetic cell in heavy lines. (b) shows the proposed order of chains in the 1/3 magnetisation phase, based on a $\sqrt{3}\times\sqrt{3}$ superstructure of the basic hexagonal vectors (broken lines). The predicted magnetic supercell is drawn in heavy lines and the supercell vectors are given in the text.

are perpendicular to *b* in CoV_2O_6. The same *ab*-plane spin order was reported for triclinic CuV_2O_6, but the interchain alignment in the *c*-direction was unclear [11]. The observed magnetic structure of monoclinic CoV_2O_6 confirms that the intrachain interactions are ferromagnetic, in keeping with the positive value of θ, and with previous results for triclinic CoV_2O_6 although here the incommensurate long-range spin-ordered structure has not yet been determined [3].

The zero-field magnetic structure of monoclinic CoV_2O_6 is antiferromagnetic as there are equal numbers of spin-up and spin-down chains parallel to *b*. Each chain is connected through Co–O–V–O–Co pathways to six neighboring chains, with antiferromagnetic couplings to four chains (at $\pm a/2$ and $\pm c$) and ferromagnetic coupling to the other two (at $\pm(a/2+c)$). The six neighbors are arranged in an approximately hexagonal arrangement around each chain, and the hexagonal representation (Fig. 6) is useful for considering the likely spin order in the 1/3 magnetisation plateau phase observed when a moderate field is applied to CoV_2O_6. The $a\times b\times 2c$ zero-field magnetic cell contains two spin-up and two spin-down chains, as shown in Fig. 6a. The 1/3 magnetisation phase has to contain two spin-up chains for each spin-down chains, and the simplest way to achieve this on a hexagonal lattice is through a $\sqrt{3}\times\sqrt{3}$ superstructure of the basic hexagonal vectors, as shown on Fig. 6b. On the monoclinic CoV_2O_6 lattice this order generates the magnetic supercell with vectors $a_m=a+c$, $b_m=b$, and $c_m=3c$ that is also shown. High field neutron diffraction experiments will be needed to test whether this spin structure is observed in the 1/3 magnetisation plateau region of monoclinic CoV_2O_6 and in other brannerites showing the same feature.

Acknowledgments

We thank the EPRSC and the Leverhulme Trust for support. We also thank STFC for access to neutron diffraction facilities at ISIS and Dr. Kevin Knight for assistance with the experiment.

References

[1] M. Hase, M. Kohno, H. Kitazawa, N. Tsuji, O. Suzuki, K. Ozawa, G. Kido, M. Imai, X. Hu, Phys. Rev. B 73 (2006) 104419.
[2] K. Okamotoa, A. Kitazawa, J. Phys. Chem. Solids 62 (2001) 365–368.
[3] S.A.J. Kimber, H. Mutka, T. Chatterji, T. Hofmann, P.F. Henry, H.N. Bordallo, D.N. Argyriou, J.P. Attfield, Phys. Rev. B 84 (2011) 104425.
[4] S.A.J. Kimber, J.P. Attfield, Phys. Rev. B 75 (2007) 064406.
[5] Z. Chuan-Cang, L. Fa-Min, D. Peng, C. Lu-Gang, Z. Wen-Wu, Z. Huan, Chin. Phys. B 19 (6) (2010) 067503.
[6] K. Mocala, J. Ziolkowski, J. Solid State Chem. 69 (1987) 299–311.
[7] M. Belaiche, M. Bakhache, M. Drillon, A. Derrory, S. Vilminot, Phys. B 305 (2001) 270–273.
[8] B. Jasper-Tonnies, H. Muller-Buschbaum, Z. Anorg. Allg. Chem. 508 (1984) 7–11.
[9] K. Singh, A. Maignan, D. Pelloquin, O. Perez and Ch. Simon, J. Mater. Chem.. (2012) 10.1039/c2m16290c.
[10] C. Calvo, D. Manolescu, Acta Cryst. B 29 (1973) 1743.
[11] A.N. Vasilev, L.A. Ponomarenko, E.V. Antipov, Yu.A. Velikodny, A.I. Smirnov, M. Isobe, Y. Ueda, Phys. B 284-288 (2000) 1615–1616.
[12] J. Kikuchi, K. Ishiguchi, K. Motoya, M. Itoh, K. Inari, N. Eguchi, J. Akimitsu, J. Phys. Soc. Jpn. 69 (2000) 2660–2668.
[13] A.V. Prokofieva, R.K. Kremerb, W. Assmus, J. Cryst. Growth 231 (2001) 498–505.
[14] M. Gondrand, A. Collomb, J.C. Joubert, R.D. Shannon, J. Solid State Chem. 11 (1974) 1–9.
[15] M. Lenertz, J. Alaria, D. Stoeffler, S. Colis, A. Dinia, J. Phys. Chem. C 115 (2011) 17190–17196.
[16] A.C. Larson and R.B. Von Dreele, Los Alamos National Laboratory Report no. LAUR 86-748 (1994) (unpublished).
[17] I.D. Brown, D. Altermatt, Acta Crystallogr. B41 (1985) 244–247.
[18] O. Mentre, F. Bouree, J. Rodriguez-Carvajal, A. El Jazouli, N. El Khayati, El M. Ketatni, J. Phys.: Condens. Matter 20 (2008) 415211.
[19] J.M. Rojo, J.L. Mesa, L. Lezama, J.L. Pizarro, M.I. Arriortua, J. Rodriguez Fernandez, G.E. Barberis, T. Rojo, Phys. Rev. B 66 (2002) 094406.